



Ultra-elastic recovery and low friction of amorphous carbon films produced by a dispersion of multilayer graphene

Junyan Zhang^{*}, Bin Zhang, Qunji Xue, Zhou Wang

State Key Laboratory of Solid Lubrication, Lanzhou Institute of Chemical Physics, Chinese Academy of Sciences, Lanzhou 730000, China

ARTICLE INFO

Article history:

Received 27 December 2010
 Received in revised form 5 December 2011
 Accepted 13 December 2011
 Available online 5 January 2012

Keywords:

Magnetron sputtering
 Grapheme
 Friction coefficient
 Elastic recovery

ABSTRACT

Hydrogenated carbon films with embedded multilayer graphene were prepared by magnetron sputtering a Ni target in methane. The films demonstrate ultra-elastic recovery (81%) and low friction coefficient (0.06), in contrast with films that did not contain graphene, whose elastic recovery and friction coefficient are 50% and 0.12, respectively. The excellent mechanical properties were attributed to the presence of multilayer-graphene embedded in amorphous carbon matrix.

© 2012 Elsevier B.V. All rights reserved.

1. Introduction

The mechanical and tribological behaviors of carbon films are not only related to bonding configuration, but also dominated to some extent by microstructure. Our recent work has shown that the introduction of carbon allotropes, such as fullerene, nanotube and expanded graphite, could decrease the internal stress and increase the hardness and elasticity of amorphous carbon films [1–3]. The presence of fullerene-like structure brought ultra high elasticity and super low friction to amorphous carbon films [4,5].

Graphene is the two-dimensional building block for carbon allotropes of every other dimensionality. It was predicted to have a range of unusual properties, such as electronic properties, thermal conductivity, mechanical stiffness and high elasticity [6]. If graphenes are introduced into carbon films, we deduce that the graphene contained amorphous carbon films may possess interesting properties. It was verified in our previous work that the incorporation of multilayer graphene oxide sheets into amorphous carbon films by liquid process showed an improved hardness and elastic recovery [3]. However, amorphous carbon and graphene are normally grown by different methods, so the growth of graphene contained amorphous carbon structures by chemical or physical vapor deposition is a challenge. Encouragingly, it is well known that, noble metals (Ru, Pt and Ni) were extensively used as catalysts for the deposition of graphene layers [7,8]. In the present work, graphene-like structures were intentionally grown on

the Ni target surface firstly and then sputtered off to deposit onto Si substrate to form graphene embedded amorphous carbon films. The graphene embedded amorphous carbon films showed both ultra-elastic recovery (81%) and low friction coefficient (0.06).

2. Experimental

2.1. Film deposition

Prior to the deposition, a base pressure of 4.0×10^{-3} Pa was attained. Then methane (99.99%) was introduced into the chamber as the plasma source and the reactive gas. The gas pressure was kept at 0.4 Pa during the whole experimental process. In the first step, the substrate holder backed against the Ni target. A layer of carbon film (Fig. 1) was grown firstly on the Ni (99.6%) target surface to prevent Ni from being sputtered out (by sputtering Ni target in methane for 5 min, with sputtering power of about 1000 W and the target surface area of $28 \text{ cm} \times 8 \text{ cm}$). Then the substrate holder was turned to the Ni target covered by a carbon layer with a distance of 100 mm. The carbon films were then deposited on silicon (N (100)) substrates at the same conditions except with a lower bias voltage (100 V). The substrate temperature could rise up to about 150 °C in 10 min due to the plasma heating effect, and never surpassed 165 °C (measured by a thermo-couple) during whole deposition process. Amorphous carbon film was deposited by sputtering a graphite target in methane as comparison. Both kinds of the films with thickness of about 1.2 μm were obtained after 100 min deposition, measured by a surface profilometer at a step formed on the film by masking the substrate.

^{*} Corresponding author. Tel./fax: +86 931 4968295.

E-mail addresses: junyanzh@yahoo.com (J. Zhang), zhangbin707245@163.com (B. Zhang).

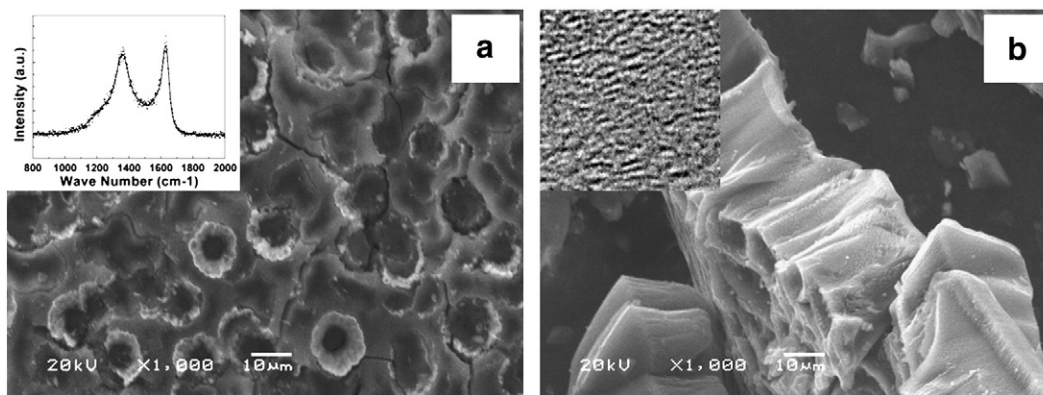


Fig. 1. Plane-view FESEM image and the corresponding Raman spectrum (a), and cross-section FESEM image and the corresponding HRTEM image (b) of the films scratched off from Ni target.

2.2. Structural characterization and mechanical property test

A JEOL JSM-6701F field emission scanning electron microscope (FESEM) was employed to examine the morphology of the films growing on Ni target. The microstructures of the specimens were observed using a JEM-3010 high resolution transmission electron microscope (HRTEM) at an accelerating voltage of 300 kV, equipped with energy dispersive spectrum (TEM-EDS). The samples with thicknesses up to 50 nm, for HRTEM analysis, were grown on freshly cleaved NaCl wafers followed by the dissolution of the NaCl wafers with water. Raman spectra of all samples were measured with a LAB-RAM HR 800 micro-Raman spectrometer at wavelength of 532 nm (2.3 eV). The chemical composition of the films was determined by a PHI-5702 multifunctional X-ray photoelectron spectroscopy (XPS), with Al K α radiation (photo energy 1476.6 eV) as the excitation source. The energy analyzer was set such that the Au (4f7/2) line was recorded as reference with a full width at half maximum of 0.9 eV. The loading–unloading displacement curves of the films were measured by a nanoindenter (Hysitron TriboIndenter, USA) with a Berkowich diamond tip. Five replicated indentations were made for each sample and the hardness was calculated from the loading–unloading curves. The elastic recovery was calculated using the formula $R = (d_{\max} - d_{\text{res}}) / d_{\max}$ [9], where d_{\max} and d_{res} are the maximum and minimum displacements during loading and unloading, respectively. The friction behaviors were evaluated on a commercial reciprocating ball-on-disk tribometer (UMT-2MT, USA) with a mating ball of uncoated Si $_3$ N $_4$ with a diameter of 3 mm. All tests were performed under a load of 2 N, the amplitude 2.5 mm, the frequency 10 Hz and the relative humidity about 40%.

3. Results and discussion

3.1. Composition and structure analyses of the films

The plane and cross-section FESEM images of the carbon films grown on Ni target (Fig. 1) show a porous structure. The inserted Raman spectrum (Fig. 1a) with two sharp peaks implies that the grown film is highly ordered [10]. Two second-order Raman peaks centered at 2700 and 3200 cm $^{-1}$, corresponding to the 2D and 2G vibration, also appear, indicating the presence of ordered structures [11]. The HRTEM image (Fig. 1b) indicates that the films grown on target surface are layered structure [12].

The plane-view HRTEM image of the carbon films deposited on NaCl substrate by sputtering Ni target in methane (Fig. 2a) indicates that some crystals dispersed in amorphous carbon matrix. Typical XPS spectrum of the carbon films deposited onto Si substrate by sputtering the layered carbon films covered on Ni target in methane are shown in Fig. 2b, in which Au, C and O were all detected. The

Ni2p3/2 and Ni2p1/2 peaks at the binding energy of 857.2 and 874.1 eV, respectively, are not observed, implying that the Ni content in films is very low. The appearance of O1s peak can be designated to the contamination of the sample exposed to air and the residual gas in the chamber, while Au coming from the pretreatment process which is often used for calibration in XPS analysis. Combined with the XPS result, it can be concluded that the dispersed nanocrystals in the amorphous carbon matrix are carbon-based crystals instead of Ni. The lattice fringes of curved plane with a plane spacing about 3.5 Å in the upper circle, corresponding to the graphite d_{002} spacing [13], can be observed. While in the lower one, nanocrystal with lattice distance of 2.45 Å can be recognized as in-plane graphene-layers [14]. The corresponding selected area electron diffraction (SAED) patterns (Fig. 2b) resemble those of amorphous carbon or graphite, besides some diffraction image points matching well with interplanar spacing of 2.43 Å in graphene layer [14]. Until now, it is clearly verified that the embedded nanocrystals in amorphous carbon film are multilayer graphene though the growth time was short. Fig. 3c and d show the typical HRTEM image and the corresponding SAED patterns of the carbon film deposited on NaCl substrate by sputtering graphite target in methane where no graphene-layers are observed.

In order to get further confirmation of above conclusions from the films deposited on NaCl, the as-deposited films on Si substrates were scratched off for HRTEM observation. As shown in Fig. 4a and b, some crystals can be observed (Fig. 3a) dispersing in carbon matrix. The SAED pattern shows the six-fold rotational symmetry expected from the diffraction with the beam incident along [0001] (Fig. 3a). The first five sets of spots correspond to d-spacing (Å) of 4.24, 2.51, 2.18, 1.45 and 1.26. The samples scratched off from the substrate were ultrasonic dispersion in acetone for 10 min and some crystals isolated from the matrix also employed for HRTEM tests. Crystals with several hundred nanometers can be seen (Fig. 3b). The typical image in Fig. 4b clearly shows stacking steps, with an interplanar spacing of 2.45 Å clearly observed. As the Ni target was completely covered by graphene-like structure which contained only a few amount of nickel, the possibility of the existence of Ni or Ni $_3$ C is ruled out (Fig. 2b). Stankovich et al. obtained patterns of polystyrene-graphene composite, confirmed to arise from individual graphene-based sheet, giving a series of d-spacing of 4.23, 2.45, 2.12, 1.42 and 1.23 [3,15]. Therefore it can be confirmed that these crystals are in plane graphene-layers. Besides, a Moire pattern can be clearly seen from HRTEM image (Fig. 3b). The average distance between the neighboring Moire patterns is 7.5 Å, that is, 3 times the lattice constant of graphene. Moire patterns have been observed on top layer of highly oriented pyrolytic graphite using the scanning tunneling microscopy [16], and more recently it has been observed frequently on few-layer (multilayer) graphene using both the scanning tunneling microscopy and HRTEM [17–19]. It is believed that Moiré patterns

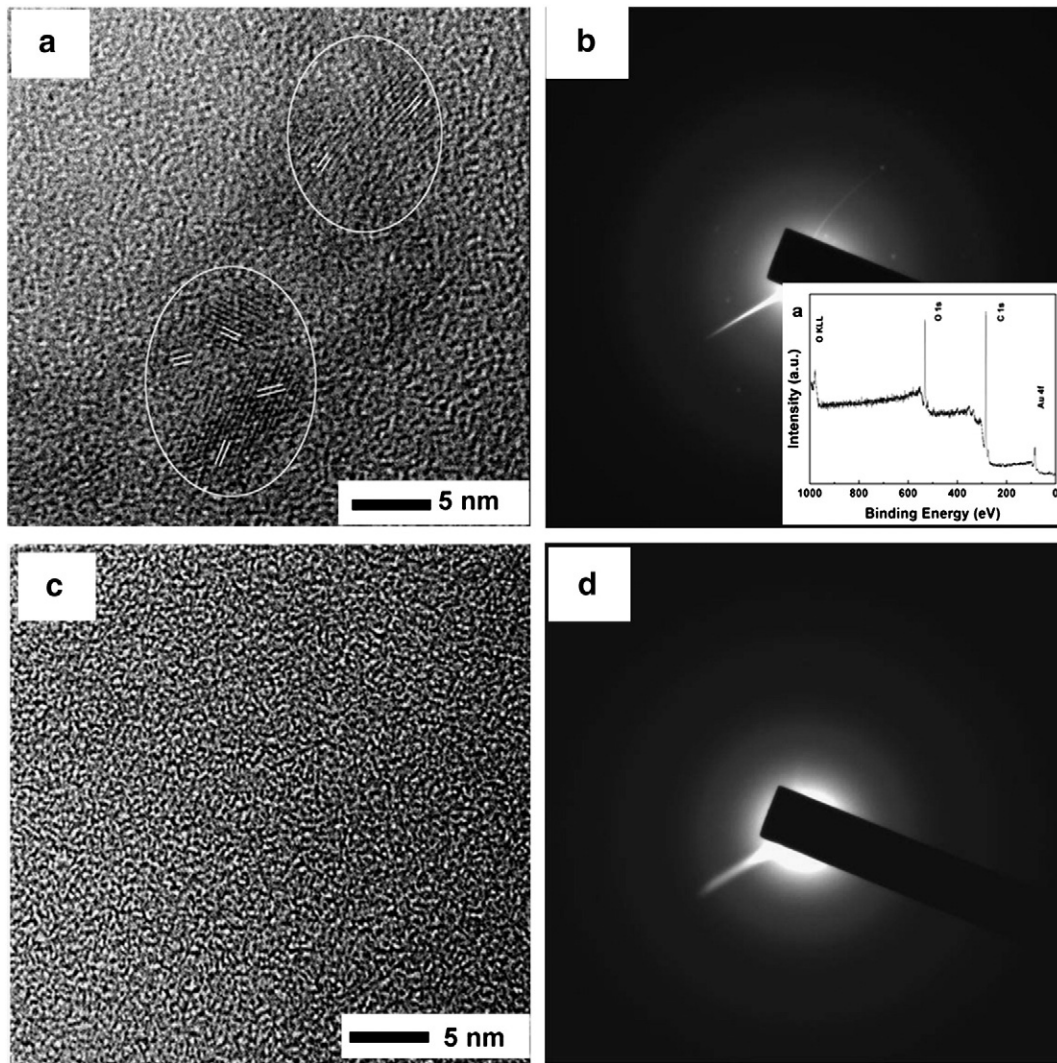


Fig. 2. HRTEM image (a) and the corresponding SAED patterns and XPS spectrum (b) of the carbon film deposited on NaCl substrate by sputtering Ni target in methane, and HRTEM image (c) and the corresponding SAED patterns (d) of the carbon film deposited on NaCl substrate by sputtering graphite target in methane.

arise from the misoriented of graphene layer. The periodicity D of a Moiré pattern arising from a rotational angle θ between hexagonal lattices is $D = 2.46/2\sin(\theta/2)$ [16]. For the measured value, 7.5 Å, the rotation angle is 19.2° in present study.

Raman spectrum of the multilayer graphene embedded amorphous carbon film is shown in Fig. 3c where two intense peaks can be clearly seen, but cannot be fitted by two Gaussian peaks. Acceptable fitting could be reached with three Gaussian lines at about 1387, 1568 and 1622 cm^{-1} (Fig. 3d). The first two peaks, typical bands of carbon based films, correspond to atomic displacements of the graphitic disorder mode and E2g mode, respectively. What is the source of the peak at 1622 cm^{-1} ? Generally, microcrystalline graphite, carbon nanowalls, carbon nanotubes and graphene, all have an additional peak at 1620 cm^{-1} [20,21] due to the terminated graphene-layers and the asymmetry of the layer planes appeared at the edges. It was also suggested that the peak at 1630 cm^{-1} was observed for nanocrystal diamond, assigned to the localized 100 sp^2 bonded pairs of carbon atoms [22]. The peak at 1620 cm^{-1} is very well known in the graphene community, Ferrari et al. [23] and Casiraghi et al. [24] believed that the peak at 1620 cm^{-1} aroused from the disorder and defects of graphenes. Thus, in our present work, the origin of 1622 cm^{-1} peak can be attributed to the disorder and defects of graphenes. Two second-order Raman peaks centered at 2700 and 3200 cm^{-1} , corresponding to the 2D and 2G vibration, also appear,

indicating the presence of ordered structures [11]. This further provides the evidence of multilayer graphene in amorphous carbon matrix.

3.2. Mechanical properties

Fig. 4a shows the load–unload displacement curves of the amorphous carbon film with and without embedded multilayer graphene. The elastic recovery was calculated using the formula $R = (d_{\text{max}} - d_{\text{res}})/d_{\text{max}}$ [9]. Noticeably, R is as high as 81% with a hardness of 6.83 GPa for the amorphous carbon film with embedded multilayer graphene; while R is only 50% with a hardness of 5.33 GPa for the amorphous carbon film without embedded graphene. It was reported that the graphenes have excellent mechanical properties, especially high elasticity (nearly 100%) [25–27]. Thus, the excellent performances in the elasticity and hardness of the film with graphene are bestowed to the presence of the multilayer graphene in amorphous carbon matrix [3]. The film with graphene shows relatively steady friction behavior with friction coefficient of 0.06, much lower than that of the film without graphene, 0.12 (Fig. 4b).

4. Conclusions

In conclusion, the graphene/amorphous carbon composite films can be prepared by magnetron sputtering Ni target in methane. The

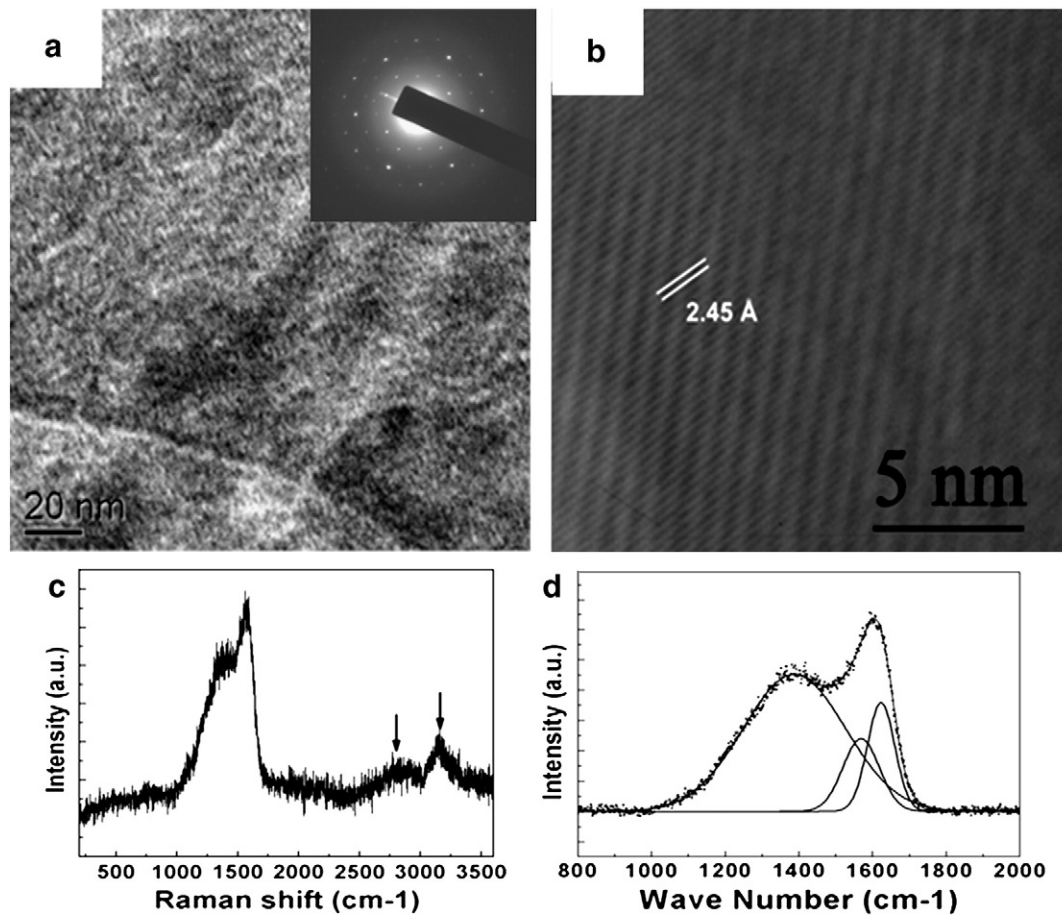


Fig. 3. TEM images of the scratched off carbon film deposited by sputtering Ni target in methane. Low magnified image and the corresponding SAED patterns (a) of the nanostructure films grown on Si substrates, and corresponding samples, HRTEM image after ultrasonic dispersion in acetone for 10 min (b); Raman spectrum of the nanostructure films grown on Si substrates (c, d).

multilayer graphene structure was generated from the decomposition of methane on Ni target which is usually used as catalyst to fabricate graphene, and then the multilayer graphene were sputtered out and grew up into carbon matrix on Si substrate due to the annealing effect of plasma. This unique structure of the films restrains plastic deformation, which in turn assists the relaxation of stress, and thus enhances the mechanical properties. With ultra-elastic recovery (81%), low hardness (6.83GPa) and low friction coefficient (0.06), the

graphene/amorphous carbon composite films may be used for the protection of flexible substrate.

Acknowledgments

The project was supported by “863” program (No. 2007AA03Z338) of the Ministry of Science and Technology of China and National Natural Science Foundation of China (Nos. 50823008, 50975273).

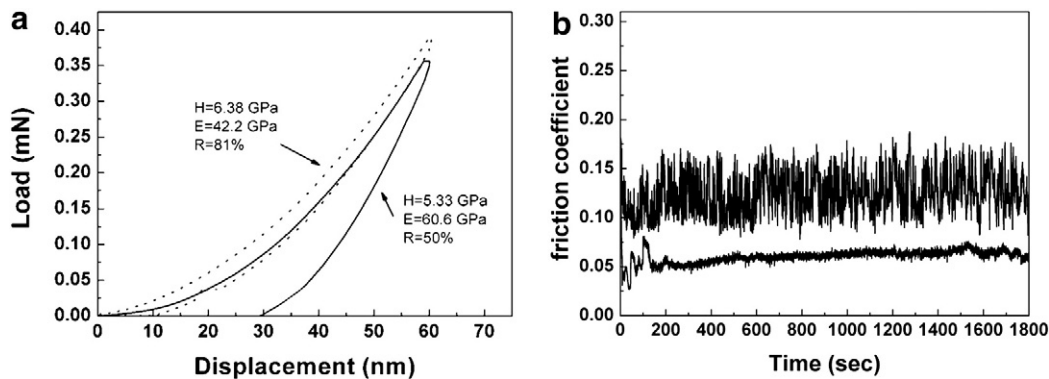


Fig. 4. Nanoindentation load–displacement curves (a), and friction coefficients (b) of the carbon film sputtered deposition by sputtering Ni (dot line) and graphite target in methane (solid line).

References

- [1] H. Hu, G. Chen, J. Zhang, *Surf. Coat. Technol.* 202 (2008) 5943.
- [2] H. Hu, G. Chen, J. Zhang, *Carbon* 46 (2008) 1095.
- [3] J. Zhang, Y. Yu, D. Huang, *Solid State Sci.* 12 (2010) 1183.
- [4] Q. Wang, C. Wang, Z. Wang, J. Zhang, D. He, *Appl. Phys. Lett.* 91 (2007) 141902.
- [5] C. Wang, S. Yang, Q. Wang, Z. Wang, J. Zhang, *Nanotechnology* 19 (2008) 225709.
- [6] A.K. Geim, K.S. Novoselov, *Nat. Mater.* 6 (2007) 183.
- [7] S. Marchini, S. Günther, J. Wintterlin, *Phys. Rev. B* 76 (2007) 075429.
- [8] S. Fan, M.G. Chapline, N.R. Franklin, T.W. Tomblor, A.M. Cassell, H. Dai, *Science* 283 (5401) (1999) 512.
- [9] W.T. Zheng, H. Sjöström, I. Ivanov, K.Z. Xing, E. Broitman, W.R. Salaneck, et al., *J. Vac. Sci. Technol., A* 14 (5) (1996) 2696.
- [10] F. Tuinstra, J.L. Koenig, *J. Chem. Phys.* 53 (1970) 1126.
- [11] Z. Luo, T. Yu, K.-J. Kim, Z. Ni, Y. You, S. Lim, et al., *ACS Nano* 3 (7) (2009) 1781.
- [12] G. Eda, G. Fanchini, M. Chhowalla, *Nat. Nanotechnol.* 3 (2008) 270.
- [13] Y. Xu, H. Bai, G. Lu, C. Li, G. Shi, *J. Am. Chem. Soc.* 130 (18) (2008) 5856.
- [14] H.L. Sun, Q.T. Shen, J.F. Jia, Q.Z. Zhang, Q.K. Xue, *Surf. Sci.* 542 (2003) 94.
- [15] S. Stankovich, D.A. Dikin, G.H.B. Dommett, K.M. Kohlhaas, E.J. Zimney, E.A. Stach, et al., *Nature* 442 (2006) 282.
- [16] J. Xhie, K. Scatter, M. Ge, N. Venkateswaran, *Phys. Rev. B* 47 (1993) 15835.
- [17] J. van den Brink, *Nat. Mater.* 9 (2010) 291.
- [18] J.H. Warner, M.H. Rummeli, T. Gemming, B. Buchner, G.A.D. Briggs, *Nano Lett.* 9 (2009) 102.
- [19] J.H. Warner, F. Schaffel, M.H. Rummeli, B. Buchner, *Chem. Mater.* 21 (12) (2009) 2418.
- [20] T. Livneh, T.L. Haslett, M. Moskovits, *Phys. Rev. B* 66 (2002) 195110.
- [21] J.O. Orwa, K.W. Nugent, D.N. Jamieson, S. Praver, *Phys. Rev. B* 62 (2000) 5461.
- [22] K.N. Kudin, B. Ozbas, H.C. Schniepp, R.K. Prudhomme, I.A. Aksay, R. Car, *Nano Lett.* 8 (1) (2008) 36.
- [23] A.C. Ferrari, *Solid State Commun.* 47 (2007) 143.
- [24] C. Casiraghi, A. Hartschuh, H. Qian, S. Piscanec, C. Georgi, *Nano Lett.* 9 (4) (2009) 1433.
- [25] C.G. Lee, X. Wei, J.W. Kysar, J. Hone, *Science* 321 (2008) 385.
- [26] Y. Gao, P. Hao, *Physica E* 41 (2009) 1561.
- [27] M. Poot, H.S.J. van der Zant, *Appl. Phys. Lett.* 92 (2008) 063111.